Xue and Gao *Applied Biological Chemistry* (2024) 67:55
https://doi.org/10.1186/s13765-024-00904-8

KSABC
The Korean Society for Applied Biological Chemistry

ARTICLE Open Access

Novel fabrication of macromolecular multi-functional hydrogel encapsulated with HUCB-derived mesenchymal stem cells to effective regeneration of cardiac repair after acute myocardial infarction

Jun Xue[1] and Yu Ping Gao[1*]

Abstract
Acute myocardial infarction (AMI) has been treated via injectable hydrogels and biomaterial patches invented using tissue engineering advancements over the past decade. Yet the curative potential of injectable hydrogels and stem cells is limited. Here, we propose the development of an injectable and conductive hydrogel composed of oxidised macromolecular hyaluronic acid and chitosan-grafted aniline tetramer polymeric components. In an attempt to enhance the therapeutic potential of AMI therapy, mesenchymal stem cells derived from human umbilical cord blood (HUCB-MSC) have been integrated into the formulation of a conductive hydrogel. For reliable connection to the beating hearts, the hydrogel exhibited suitable adhesive properties. Hydrogel's potent biocompatibility was determined by in vitro investigations of cell viability and proliferation of NRCMs and H9C2 cardiomyocytes. After myocardial injection, longer HUCB-MSCs survival length, cardiac functioning, and histology in SD rat myocardium were demonstrated, greatly associated by up-regulation and downregulation of cardiac-related relative gene expressions of angiogenic factors and inflammatory factors, respectively. The injectable hydrogel that contained HUCB-MSCs substantially enhanced the therapeutic benefits, indicating a potentially beneficial therapeutic approach to AMI therapy.

Keywords Acute myocardial injection, Cell delivery, Injectable hydrogel, Stem cell therapy, Cell proliferation, In vivo rat model

*Correspondence:
Yu Ping Gao
Dr.JasperG@outlook.com
[1]Department of Vasculocardiology, Tongji Shanxi Hospital, Shanxi Bethune Hospital, Shanxi Academy of Medical Sciences, Third Hospital of Shanxi Medical University, Taiyuan 030032, PR China

Introduction

Heart failure and myocardial infarction (MI) continue to be the primary causes for mortality around the world. High rates of mortality and incapacity from cardiovascular disease remain notwithstanding current developments in pharmaceutical and medical device therapies [1, 2]. Ischemia myocardium's averse microenvironment increases considerable cell death, which in effect causes ventricular wall weakening and dilatation and lead to ultimately heart failure [3, 4]. No current therapeutic treatment, whether pharmaceutical medicines or implants, is capable of making up for the loss of cardiomyocytes (CMs) after MI, and these treatments are considered as essentially palliative rather than curative. Therefore, reducing the loss of CMs becomes essential for repairing the structure and functioning of the ischemic myocardium, and this could be accomplished by enhancing the milieu by inhibiting inflammatory reactions and stimulating angiogenesis [5, 6]. Recent research reports have provided several treatment strategies for myocardial infarction. R. A. Watson et al., suggested that the use of anti-coagulant medication, thrombolytics, and surgical intervention to restore normal blood flow are effective treatments for myocardial infarction [7]. Q. Li et al., highlights the importance of CD74 signaling in protecting the heart after injury, indicating that targeting this pathway could be a potential therapeutic strategy for myocardial infarction [8]. Furthermore, research has also shown that thymosin β4, a peptide with pleiotropic abilities, may be a promising candidate for the treatment of ischemic heart disease [9, 10]. Another potential treatment strategy for myocardial infarction involves the use of scutellarin, an herbal flavonoid glucuronide with multiple pharmacological activities. These treatment strategies aim to complement reperfusion by providing neural and cardiovascular protection, targeting multiple abnormalities in ischemia, and reducing infarct size while improving myocardial function and perfusion [11]. Additionally, there is ongoing research focused on identifying novel targets for designing newer therapeutic modalities in the treatment of myocardial infarction, as current protocols remain suboptimal. Overall, recent research reports provide a range of treatment strategies for myocardial infarction, including the use of anti-coagulant medication, thrombolytics, surgical intervention, CD74 signaling targeting, thymosin β4, and scutellarin. However, further research and clinical trials are needed to fully evaluate the efficacy and safety of these strategies in improving outcomes for patients with myocardial infarction [12–15].

Numerous kinds of stem cells (SCs) have reached to the stage of clinical testing as an acceptable approach to repair damaged tissue. The purpose of stem cell transplantation in cardiac tissue engineering is to facilitate cardiac regeneration in patients with heart injuries [16, 17]. The stem cell therapy has an unfavourable history in clinical trials because of the limited cell retention rate and the negative consequences of immunological rejection caused by the use of allogeneic cells. The paracrine mechanism of stem cell therapies has attracted significant attention as a potential treatment for various life-threatening diseases due to its crucial role in restoring the natural microenvironment in injured tissues [18, 19]. Recent research reports have shown promising developments in using stem cells for the treatment of myocardial infarction. F. Guilhot highlights the use of patient-derived induced pluripotent stem cells and human embryonic stem cells, which are pluripotent and have been used for the treatment of cardiac disorders [20]. Additionally, the use of CAR-T cells is a promising approach for treating lymphomas and myeloma. These advancements in stem cell research hold great potential for improving treatment options for patients with myocardial infarction, ultimately reducing mortality rates and improving overall cardiac function and outcomes in patients with myocardial infarction [20–22]. Emerging evidence suggests that stem cells have the potential to be mobilized and differentiate into cardiomyocytes after a myocardial infarction, offering a potential regenerative therapy for repairing damaged heart tissue. Overall, recent research reports indicate that stem cell therapy holds significant potential for the treatment of myocardial infarction. Furthermore, advancements in regenerative medicine and tissue engineering have allowed scientists to construct biological substitutes that can restore and maintain normal function in diseased and injured cardiac tissues [23–26]. Multiple types of stem cells have been investigated and tried so far in attempts at repairing the damaged myocardium, including adipose-derived stem cells [27], pluripotent stem cells [28], embryonic stem cells, and mesenchymal stem cells [29]. However, the therapeutic effectiveness of these approaches is significantly limited due to the incredibly low percentage of cell survival in the adverse milieu of myocardial infarction (MI) [30]. Biomaterials that are found to be applicable have demonstrated greater abilities for preserving cell engraftment and effectively conducting mechanical stimulation. In recent years, injectable hydrogels have been the focus of extensive study as a potential cell transport carrier among the range of biomaterials utilised in this scenario [31–33].

Injectable Hydrogels have been reported in biological investigations to enhance cardiac performance following myocardial infarction by way of LaPlace's Law (an elevated wall thickness and lowered wall stress) [34, 35]. However, recent research has highlighted the potential of injectable hydrogels as a promising therapeutic approach for myocardial infarction treatment [36, 37]. These hydrogels can provide structural support to the damaged tissue, promote angiogenesis and tissue

regeneration, and enhance cardiac function. This innovative strategy involves the injection of a bioengineered hydrogel directly into the damaged area of the heart, where it forms a scaffold that supports cell infiltration, survival, and integration [38–40]. The hydrogel acts as a temporary extracellular matrix, mimicking the natural environment of myocardial tissue and enhancing the regenerative process. The hydrogel can be customized to release therapeutic factors, such as growth factors or stem cells, which further enhance tissue regeneration and repair. Furthermore, the injectable hydrogel can be tailored to have tunable mechanical properties, allowing it to match the elasticity of native myocardium and prevent adverse remodeling. Overall, this research article highlights the potential of injectable hydrogels as a promising therapeutic strategy for myocardial infarction treatment [41–44]. Injectable chitosan-based hydrogels have been found to improve cell retention and stimulate the cardiac development of adipose-derived stem cells, according to recent studies on hydrogel materials. In the meantime, cardiac cells are in an electroactive state, reflecting the cardiovascular systems is a vital organ and has unique electrophysiological behaviours [45, 46]. It has been established that stem cells, myoblast cells, nerve cells, and heart cells, all of which respond positively to electrical stimuli, can effectively proliferate and differentiate in the presence of polymers that are conductive [47, 48]. Injectable hydrogels that possess conductivity and serve as vehicles for delivering cardiac cells are highly anticipated in the field of heart regeneration. Despite their numerous advantages, including the stimulation of cell proliferation, typical injectable conductive hydrogels could not be employed for an extended period of time with an uninterrupted function because they were not self-healing [49–52]. This emphasises the persistent need for the investigation of injectable conductive hydrogels possessing self-healing properties, which could offer advantages in the area of cardiac cellular therapy [53].

The injectable hydrogel loaded with HUCB-MSCs were designed and developed in this investigation to alleviate the multifaceted symptoms of AMI. In this study, we have effectively synthesised a range of self-healing conductive injectable hydrogels by incorporating chitosan-graft-aniline tetramer (CS-AT) with oxidised hyaluronic acid. Furthermore, we investigated the potential of these prepared hydrogels as a HUCB-MSCs delivery system for cardiac cell therapy. The hydrogels were synthesised through the combination of a solution containing CS-AT and oxidised hyaluronic acid, performed under physiological conditions. Both of these factors have the potential to greatly enhance the MI area's previously disadvantaged microenvironment. As a result of its ability to merge with cardiac tissue, it may assist HUCB-MSCs remain in the MI zone despite changes in the internal environment of the body.

Materials and methods

Materials

The chitosan powder (Mw = 100 k to 300 k), Dimethyl sulfoxide (DMSO, > 99% purity), absolute ethanol (AR grade), N, N-dimethylformamide (DMF, >99% purity), N-phenyl-1,4-phenylenediamine (aniline dimer), ferric chloride (FeCl3, >98% purity) were purchased from Sigma Aldrich (CA, USA). The cross-linking materials EDC and NHS were purchased from Aladdin Industrial Inc. PR China.

Preparation of aniline tetramer-grafted chitosan

The synthesis of aniline tetramer-grafted chitosan (AT-CS) was performed in accordance with our previously published research [54]. AT-CS was synthesised using an optimised AT content, specifically a feed ratio of 10%. In this experiment, a quantity of 0.5 g of chitosan was initially dissolved in a solution containing 50 millilitres of hydrochloric acid (HCl; 0.05 M). This process resulted in the formation of a chitosan solution with a weight% of 1%. Subsequently, a solution was obtained by dissolving 0.0916 g of EDC, 0.0550 g of NHS, and aniline tetramer (10 wt%) in freshly obtained DMF (5 mL). Afterwards, the resultant solution underwent stirring at the atmospheric temperature in order to begin the process of activation of the carboxyl group that is contained in the aniline tetramer. After a duration of 24 h, the mixture was progressively introduced into the chitosan solution at a concentration of 1% by weight. The reaction was subsequently continued for an additional 24 h. Following that, the product underwent precipitation upon the addition of a 3 M NaOH solution, followed by filtration. The precipitate was further diluted in an aqueous solution of acetic acid and (1% (v/v)) placed under centrifugation to remove the insoluble constituents. The product was rinsed with distilled water until a neutral pH was achieved. Ultimately, the product underwent a drying process within a vacuum oven for a duration of 48 h.

Synthesis of oxidized HA

Briefly, a solution containing 1.5 grammes of hyaluronic acid (HA) was entirely dispersed in DI water (150 mL). Subsequently, sodium periodate solution (16.5 mL) with a concentration of 0.25 M was introduced steadily and in gradual amounts. After 3 h of stirring at ambient temperature, the reaction was brought to a stop by adding ethylene glycol (30 mL), which was allowed to react for 1 h. Subsequently, the product underwent dialysis in DI water for 2 days, with being changed the DI water thrice daily. The HA that underwent oxidation (OHA) was obtained

through the process of freeze-drying and after that kept at a temperature of -20 °C to facilitate subsequent usage.

Fabrication of CS-AT@OHA injectable hydrogel

The prepared polymeric component of CS-AT was dissolved in an aqueous solution of acetic acid (1% (v/v)), resulting in a solution having a concentration of 3 wt%. The OHA that completed the process of freeze-drying was dissolved in a PBS medium having a pH value of 7.4. The resulting solutions contained concentrations of 3 and 6 wt%, respectively. The hydrogel formation seemed happening in just under a minute. The hydrogels, which have been produced using various CS-AT polymers, were designated as OHA@CS-AT hydrogels. The OHA@CS-AT hydrogel was synthesised through the combination of equal volumes of OHA solution and CS-AT solution.

Swelling and morphological evaluations

The evaluation of the swelling ratio of these hydrogels was performed as well. In this study, various hydrogel groups exhibiting comparable size and form were submerged in DPBS at 37 °C. Subsequently, the hydrogels were extracted at predetermined time intervals. After the removal of surplus water through the usage of filter paper, the hydrogels were then put to weighing. The swelling ratio of the hydrogels was quantified using Eq. 1, where Wt reflects the post-swelling weight of the hydrogel, and Wo refers to the pre-swelling weight of the hydrogel.

$$\text{Swelling ratio} = \frac{(w_t - w_o)}{w_o} \times 100\% \tag{1}$$

The shape and morphological structure of the injectable hydrogels were examined through the utilisation of a FE-SEM microscopic technique (Quanta S-4800, FEI). One group underwent freeze drying immediately after preparation, while another group underwent freeze drying after reaching a state of swelling equilibrium. Prior to observation, a gold sputter-coating was applied to all of the samples.

Conductivity of the hydrogel

The hydrogel samples, which have been produced with varying amounts of OHA, were utilised to investigate the conductivity ability of the injectable hydrogels. The prepared solutions of OHA and CS-AT polymeric components, with concentrations of 3 wt% and 6 wt% respectively were subjected to vortex oscillation to achieve a uniform combination. The resulting mixture was then incubated at a temperature of 37 °C for a duration of 2 h, resulting in the formation of a fully cross-linked hydrogel. Following the process of gelation, the hydrogel specimen was subsequently put into a cylindrical container. After that, the conductivity of the hydrogel was assessed using a portable conductivity meter, precisely using the HANNA8733 model.

Rheological properties of the hydrogels

The universal stress rheometer SR5 (Rheometric Scientific) was employed to conduct dynamic rheological measurements. In order to achieve a linear oscillatory deformation, the frequency for the time-sweep testing was set at 1 Hz, while the strain was set at 5%. The experiments were conducted at a temperature of 37 °C, spanning a time interval from 0 to 10 min. To investigate the dynamic properties of the hydrogels, a series of dynamic sweep tests were conducted under specific conditions. These tests were carried out in a frequency mode, with the temperature set at 37 °C and the strain applied at 5%. The frequency range for the experiments spanned from 0.1 to 50 Hz.

N Vitro degradation

The degradation rate of the hydrogel was measured using a mass loss measurement approach. Hydrogels possessing initial dry masses of 10 mg were immersed in a 10 mL solution of PBS at a temperature of 37 °C. The hydrogels were exposed to predetermined time intervals, during which they were subjected to drying and weighed using a microbalance. Subsequently, the relative mass loss was determined through calculation.

In Vitro cell viability assay

In order to assess the biocompatibility of hydrogel, a total of 1.5×10^5 neonatal rat cardiomyocytes (NRCMs) and rat cardiomyocytes (H9C2) cells were subjected to analysis using the MTT approach. The OHA@AT-CS hydrogel samples that had been sterilised were placed in the culture medium for a duration of 24 h. The cells were seeded into a 96-well plate at a density of 2×10^4 cells per well. Following this, the plate was put through incubation for a period of 24 h at a temperature of 37 °C with humidity (5% CO_2). After that, a regenerative medium consisting of 20 µL of MTT (5 mg/mL in PBS) was introduced. After a 4-h, the liquid in each well was replaced with 200 µL of dimethyl sulfoxide (DMSO). The absorbing capacity of the material at a predetermined wavelength of 570 nm was measured using a Bio-Red microplate reader. The measurement of relative cell viability was performed with the established cell survival equation. The NRCMs and H9C2 cells were exposed to a 48-h incubation period with the leaching solution obtained from the OHA@AT-CS hydrogel groups in order to conduct the Live/Dead study. Following that, the cells were stained using the acridine orange/ethidium bromide (AO/EB) staining kit in accordance with the published protocol. The cells were investigated via a fluorescent microscope (Olympus, Japan).

HUCB-derived mesenchymal stem (HUCB-MSCs) culture

The HUEB-MSCs were procured from Chinese Academy of Sciences, PR China and maintained in tissue culture dishes (100) mm using HyClone DMEM/F12 supplemented with FBS (10% (v/v)) at a temperature of 37 °C with humidity 5% CO_2. The culture medium was frequently swapped at three-day intervals. After reaching confluence, the cells went through a passage using a trypsin-EDTA (0.25%) solution.

Hydrogel encapsulation of HUEB-MSCs

HUEB-MSCs were obtained and cultured in a suitable medium. Following that, they were combined with 10× PBS and a hydrogel liquid that had been made at a concentration of 50 mg/mL. The resulting mixture was then subjected to incubation at a temperature of 37 °C, allowing for the process of gelation to begin to take place. The culture was sustained in IMDM (Invitrogen) supplemented with 20% foetal bovine serum (FBS). The morphology, cell survival, and proliferation of HUEB-MSCs in the nanogel were compared to those of HUEB-MSCs cultivated on traditional tissue culture plates (TCP). To assess cell viability, a population of 1×105 HUEB-MSCs was cultivated in 125 µL of hydrogel or on tissue culture polystyrene (TCP) within a 96-well plate for a duration of 7 days. Subsequently, the survival of the cells was determined using the live/dead viability test. The determination of cell morphology was performed based on the image analysis outcomes obtained from the ImageJ software. To assess cell proliferation, a total of 1×105 HUEB-MSCs were evenly distributed in 125 µL of hydrogel samples or on tissue culture polystyrene (TCP) within a 96-well plate. The quantification of cellular proliferation was performed at specific time points (days 1, 3, and 5) using a counting kit-8. The absorbance rate was measured using a Tecan Sunrise microplate reader, manufactured in Switzerland. The fluorescence images were acquired using a ZEISS LSM 880 microscope, manufactured by Carl in Germany.

Acute myocardial infarction model

The animal experimentation protocols adhered to the requirements set forth by the Council for the Purpose of Control and Supervision of Experiments on Animals, Ministry of Public Health, China. Furthermore, these protocols were duly authorised by the Animal Ethics and Welfare Committee of the Shanxi Medical University, PR China. The study involved conducting animal experiments on 60 male (n=30) Sprague Dawley (SD) rats (weighing 220±20 g) procured from Beijing Animal Technology Laboratory, PR China. These rats were then separated into five groups for the purpose of studying acute myocardial infarction (MI). The study consisted of five groups, each with a different treatment. Group 1, referred to as sham (n=6). Group 2, referred to as AMI (n=6), and received a treatment involving PBS. Group 3, referred to as CS-AT (n=6), and received a treatment involving 100 µL of the CS-AT hydrogel. Group 4, referred to as OHA@CS-AT (n=6), and received a treatment involving the injectable OHA@CS-AT (100 µL) hydrogel only. Lastly, Group 5, referred to as HUMSCs-OHA@CS-AT (n=6), and received a treatment involving 100 µL of the HUMSCs encapsulated OHA@CS-AT injectable hydrogel. Initially, all the rats underwent anaesthesia using isoflurane. Following that, the left-side anterior descending coronary arteries of the rats were ligated employing a 6.0 suture. The area affected by infarction exhibited a pale appearance, suggesting the successful implementation of ligation. Subsequently, developed hydrogel groups were administered via injection into the site of myocardial infarcted-induced site. The operated rat upper body were promptly stitched following the transplanting procedure. The sham group solely had thoracotomy. The animals that did not get any treatment following the surgical procedure were classified as the myocardial infarction (MI) groups. Following the surgical procedure, each rat was administered an injection of anti-biotics (penicillin) for twice daily for a duration of three days. Additionally, the provision of food and water was made available to the rats as an optional resource.

Determination of fibrosis

The fibrosis area of myocardial infarction (MI) hearts was assessed by using Masson's trichrome (MT) staining. At the end of the study, anaesthesia was administered to all rats, followed by their sacrifice 28 days post-surgery. Subsequently, the hearts of the experimental rats were extracted and immersed in a 4% paraformaldehyde solution for a duration of 48 h. Subsequently, the tissues underwent dehydration and were subsequently embedded in paraffin. After that, the heart tissues were sectioned into small slices approximately 4 µm in thickness in order to make it easier for observation of H&E and MTS staining. The slices stained with MTS were subsequently examined using a fluorescence microscope (Olympus, Japan). The fibrotic region and the thickness of the LV wall were evaluated via the ImageJ. The calculation of average percentages for the infarct areas and LV wall thicknesses was performed in three separate regions.

Statistical analysis

Means and standard deviations were used to organise the observed data. GraphPad Prism 8.0 was applied to perform a two-way analysis of variance (ANOVA) to compare the variations throughout experimental groups.

Results and discussion

To facilitate the transportation of cardiac cells, it was necessary to create a hydrogel that is injectable, conductive, and had self-healing capabilities. The selection of OHA and CS-AT polymeric materials as a constituent of our hydrogel was based on its favourable electroactivity and biocompatibility properties [55]. In order to fabricate a biocompatible hydrogel that is suitable for injection and capable of encapsulating HUCB-MSCs, the first stage was the preparation of oxidised hyaluronic acid (OHA). This was achieved by subjecting high-molecular-weight HA to oxidation using sodium periodate. Figure 1 illustrates the synthetic approach employed for the development of an OHA cross-linked CS-AT hydrogel, which holds promise as an injectable treatment for acute myocardial infarction (AMI).

The molecular structures of OHA, CS-AT, and OHA cross-linked CS-AT were confirmed by FTIR spectral examination. An obvious absorption peak at 1734 cm^{-1} was seen in the IR spectral range (Fig. 2 (a)), which was attributed to the vibration of stretching of the aldehyde group in OHA. In addition, the corresponding stretching vibrations of N=H and C=O in HA have been attributed to the identifiable absorption peaks at 1528 cm^{-1} and 1638 cm^{-1}. These findings provide evidence that the synthesis of OHA was accomplished successfully. The chemical structures of the hydrogels that were produced were confirmed through the utilisation of FT-IR spectroscopy. The observed C=C stretching vibration of the aromatic ring and amide groups (-NHCO-) in AT was confirmed by the distinctive peaks of 1575 cm-1 and 1645 cm-1 peaks noted in the CS-AT copolymer. Observations from these peaks point to an effective grafting of AT onto the polymeric chitosan components. The CS-AT hydrogel greatly attenuated the 1720 cm^{-1} aldehyde group peak. The absorption intensity ratio between the wavenumbers 1644 cm^{-1} and 1580 cm^{-1} was found to be greater in the OHA@CS-AT hydrogel compared to the CS-AT polymer, as depicted in Fig. 2 (a). The distinctive absorption of the newly formed Schiff base at 1644 cm-1 is responsible for this difference; it is the outcome of the reaction between the amine groups of CS and OHA. This research demonstrates the effective fabrication of CS-AT hydrogels. After introducing the OHA, the CS-AT hydrogel and OHA@CS-AT hydrogel solution were observed by UV spectra and exhibited the well-shown peaks at 440 and 312 nm (Fig. 2b). This was considering polarons formed in the AT segment. The peak at 800 nm, which was caused by the radical polaron, indicated that the emeraldine salts had been generated.

A great deal of research has been presented to support the belief that electroactive materials contain the ability to augment the proliferation of cells [56]. The electroactivity of the developed injectable hydrogel was assessed by the utilisation of cyclic voltammetry (CV). A four-probe method and an electrochemical workstation were employed to determine the injectable hydrogels' ability to conduct electrical activity. The CS-AT hydrogel possessed a conductivity of about 1.15×10^{-6} S/cm, as shown in Fig. 2(c). After adding 6% OHA, the CS-AT hydrogel's conductivity reached 2.80×10^{-4} S/cm (Fig. b), which was about the same as the conductivity of normal heart tissue (10^{-4} S/cm). Furthermore, it can be shown from the cyclic voltammetry (CV) curves depicted in the Figure that a rise in OHA content leads to an expansion in the size of the hysteresis loop, accompanied by a more pronounced redox peak [57]. The preceding investigation has demonstrated that the conductivity of hydrogel can be modulated by varying the concentration of OHA. The selection of CS-AT-OHA for following studies was based on its well-suited adhesion property and conductivity for cardiac patch.

The swelling behaviour of the hydrogels was investigated by submerging them in DPBS at atmospheric temperature (37°C). According to the data presented in Fig. 3 (a), it can be observed that the swelling process reached an equilibrium state after 120 minutes. At this equilibrium stage, hydrogels with varying OHA levels exhibited swelling ratios ranging from 3 wt. % to 6 wt. %. Because of the negative correlation between the cross-linking

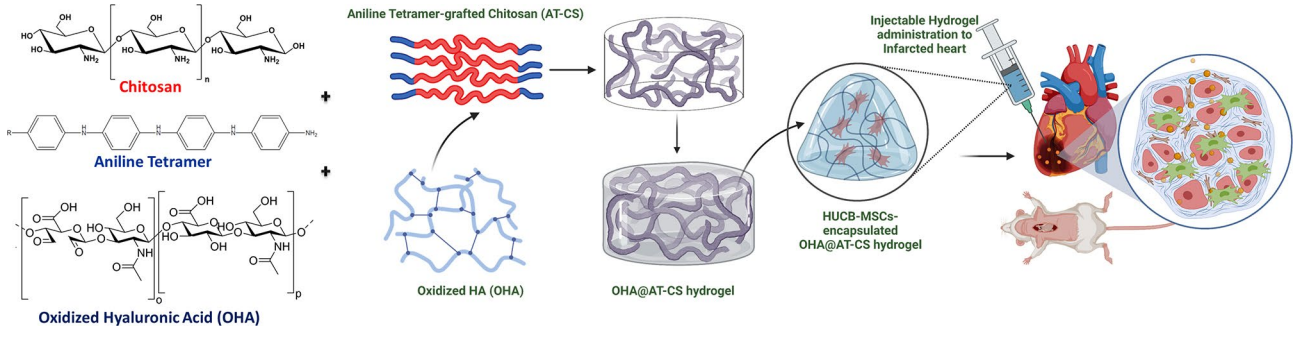

Fig. 1 Schematic representation demonstrated that fabrication of OHA-functionalized CS-AT injectable hydrogel and encapsulated with HUCB-MSC cells for the therapeutic potential of AMI therapy. Additionally, graphic presentation exhibits cell-encapsulated hydrogel structure and intracardial injection of hydrogel onto the infracted rat model

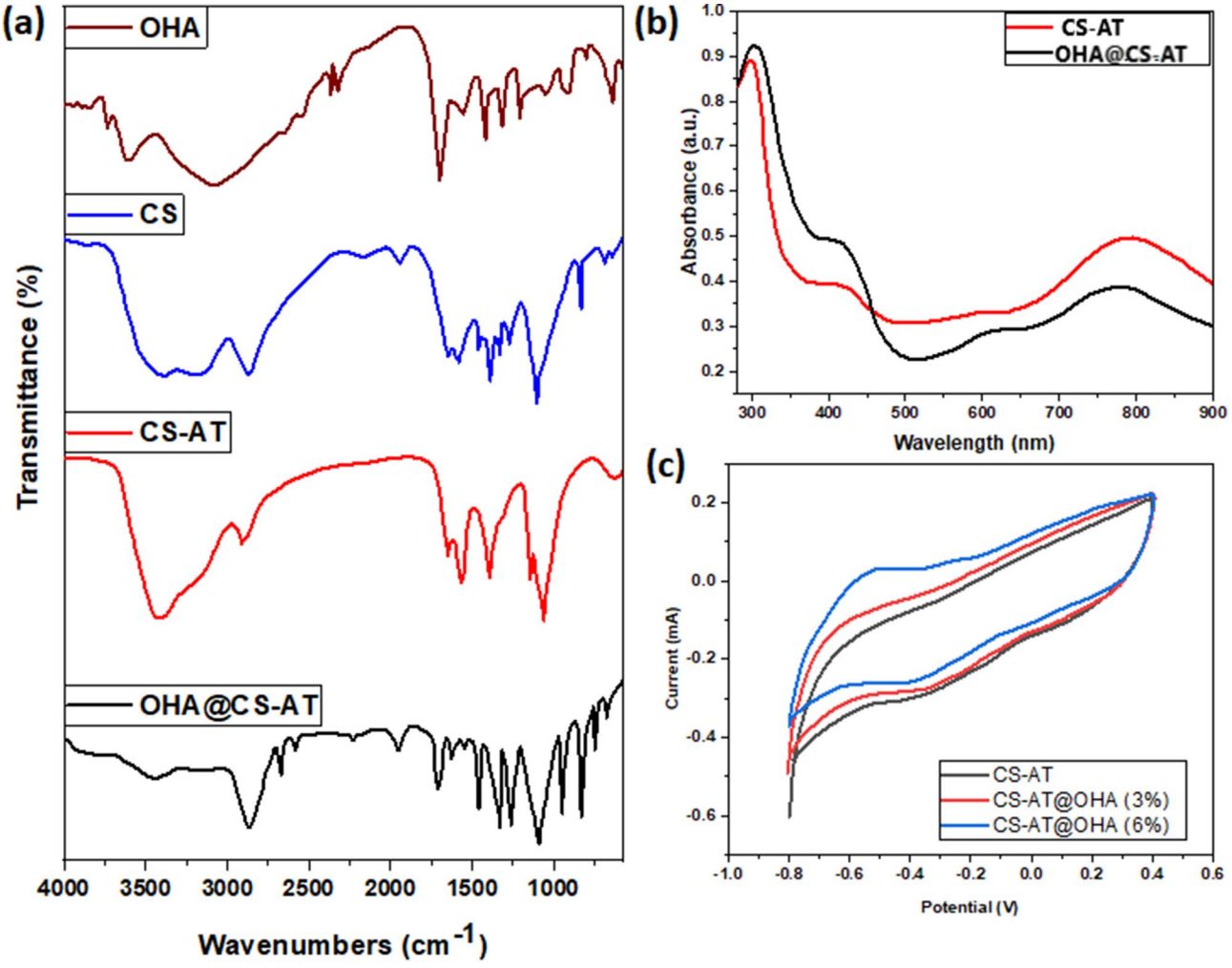

Fig. 2 Investigations on chemical structural properties, and conductivity behaviour of the prepared hydrogel samples: (**a**) Structural evaluations of OHA, CS, CS-AT and OHA@CS-AT hydrogel groups by FT-IR spectral analysis; (**b**) UV-vis analysis of CS-AT and OHA@CS-AT hydrogel materials; (**c**) Electrical conductivity analysis of the hydrogel groups with different content of OHA (3 & 6 %) by CV curve analysis

density and the OHA content, the swelling ratio of the prepared hydrogels reduced with increasing OHA concentration. The gelation performance was assessed using an inverted vial approach. As depicted in Fig. 3 (b & c), an increase in the OHA ratio (3 wt. % to 6 wt. %) resulted in accelerated gelation upon the combined action of the two constituents. Based on the findings, the reaction rate elevated when the amounts of both the aldehyde and hydrazine groups were increased. In the following steps, the hydrogels' viscoelastic characteristics were determined. The G' values exhibited larger values compared to the G" values, and an increase in the OHA ratio resulted in an increase in the hydrogel modulus from 200 to 1000 Pa (Fig. 3b). This result presents evidence that the addition of acylhydrazone linkages was caused by the interaction between aldehydes and hydrazine groups [58, 59]. The injectable hydrogel stability was also investigated through using a frequency sweep mode, as shown in Fig. 3(c). Across the entire frequency range, the OHA@CS-AT hydrogel group storage modulus (G') indicated greater values than the loss modulus (G"), demonstrating stability and revealing viscoelastic activity.

Figure 3 (d, e & f) illustrates the morphology of the prepared injectable hydrogel as examined by FE-SEM, which could shed light on the relationship between the cross-linking density and OHA concentration. The augmentation of the OHA content resulted in a corresponding enlargement of the pore size. Additionally, it was observed that the pore size of the hydrogels in their swollen state was almost twice as large as that of the hydrogels in their initial dried state. The presence of sizable pores within the hydrogels facilitates ample room for cellular migration, proliferation, and intercellular communication [60–62]. This research conducted for a Lap-shear test on porcine cardiac and skin samples to evaluate the adhesive strength of the OHA@CS-AT hydrogel. Figure 3(g) and

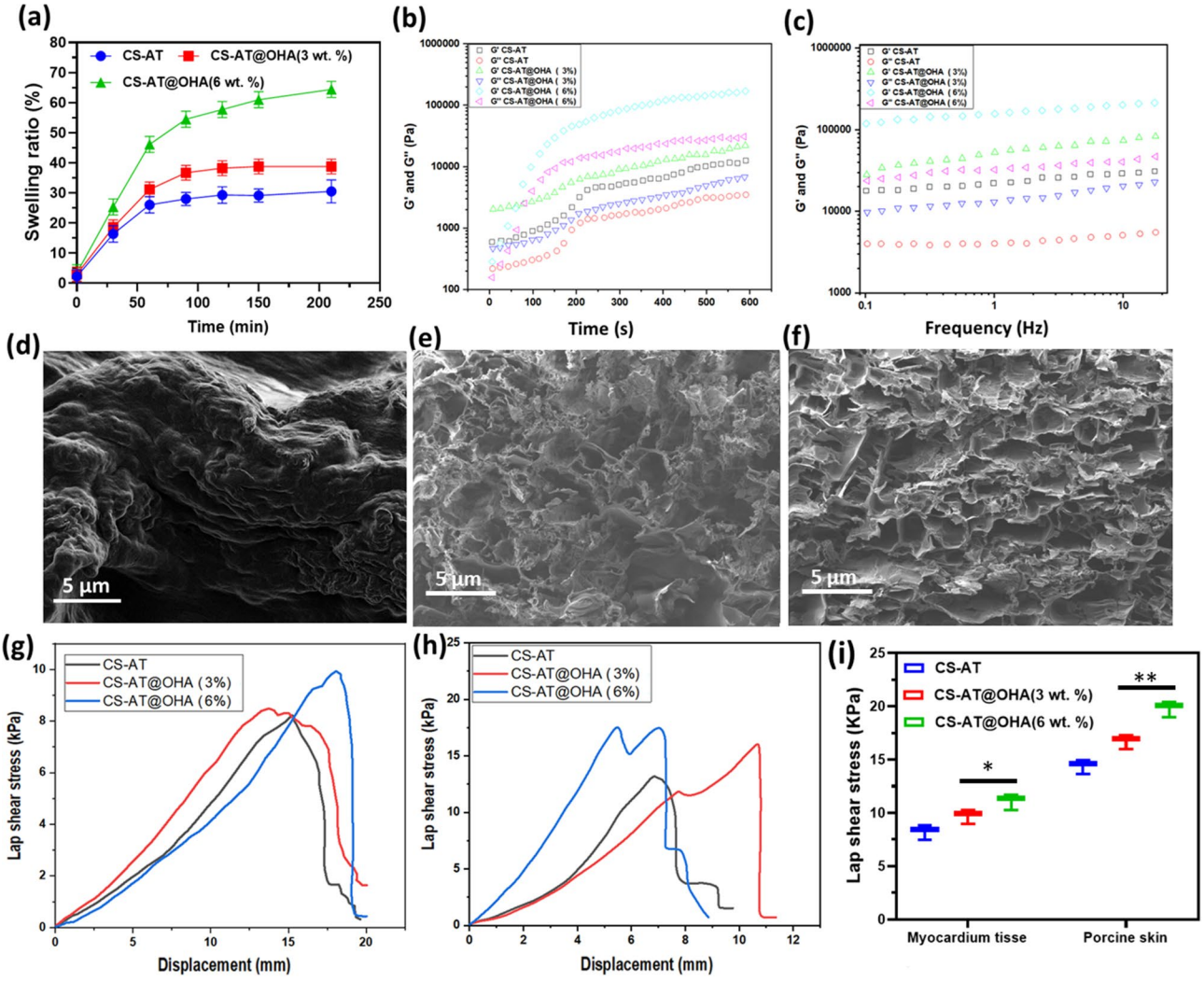

Fig. 3 Physiological, morphological and mechanical investigations of the prepared hydrogel groups: (**a**) Swelling abilities of the prepared hydrogel groups with different content of OHA (3 & 6 %); (**b**) Rheological evaluations of the prepared hydrogel groups in a time sweep mode at 37 °C; (**c**) Frequency sweep analysis of hydrogel groups in a frequency ranges from 0.1 to 20 Hz at 37 °C; (**d**, **e** & **f**) Morphological observations of developed hydrogel groups (CS-AT and CS-AT@OHA (3 & 6 wt. %)) by FE-SEM technique; (**g**, **h** & **i**) Adhesion mechanical strength of prepared hydrogel groups (CS-AT, CS-AT@OHA (3 %) and CS-AT@OHA (6 %)) to the porcine myocardial tissue and porcine skin samples. n = 3 independent experiments per group; *, ** and *** indicate $p < 0.05$, 0.01 and 0.001, respectively

(h) show that the adhesion strength of the CS-AT-OHA sample improved with increasing OHA content. As stated in Fig. 3 (g, h, & i), the adhesion strengths of the prepared injectable hydrogel to porcine cardiac tissue and porcine skin were measured to be 10 and 18 kPa, respectively. The strong adherence of the CS-AT-OHA hydrogel can be attributed to the substantial non-covalent binding capacity of the HA components to moist tissues. The CS-AT-OHA hydrogel, when applied to the myocardial tissue, demonstrated resilience to various mechanical stresses such as twisting, bending, water immersion, and forceful water flushing at a flow rate of 0.57 m/s. Notably, the gel patch remained securely attached without any instances of detachment, as depicted in the accompanying figure. This finding suggests that the CS-AT-OHA hydrogel patch exhibits robust adherence to cardiac tissue.

Previous studies have shown that both polyaniline and aniline oligomers exhibit the capability to increase the proliferation capacity of electrically responsive cells, including mesenchymal stem cells, C2C12 myoblasts, neuronal cells, and H9C2 cardiac cells [28, 63, 64]. The hydrogels known as CS-AT demonstrated favourable electroactivity and conductivity properties, which are expected to positively influence cell growth. Prior to conducting in in vivo studies, the hydrogels conducted screening to evaluate their cytotoxicity and biodegradability. The results presented in Fig. 4 demonstrate that the viabilities of NRCMs cells and H9C2, when treated with the CS-OT and CS-AT-OHA hydrogel groups,

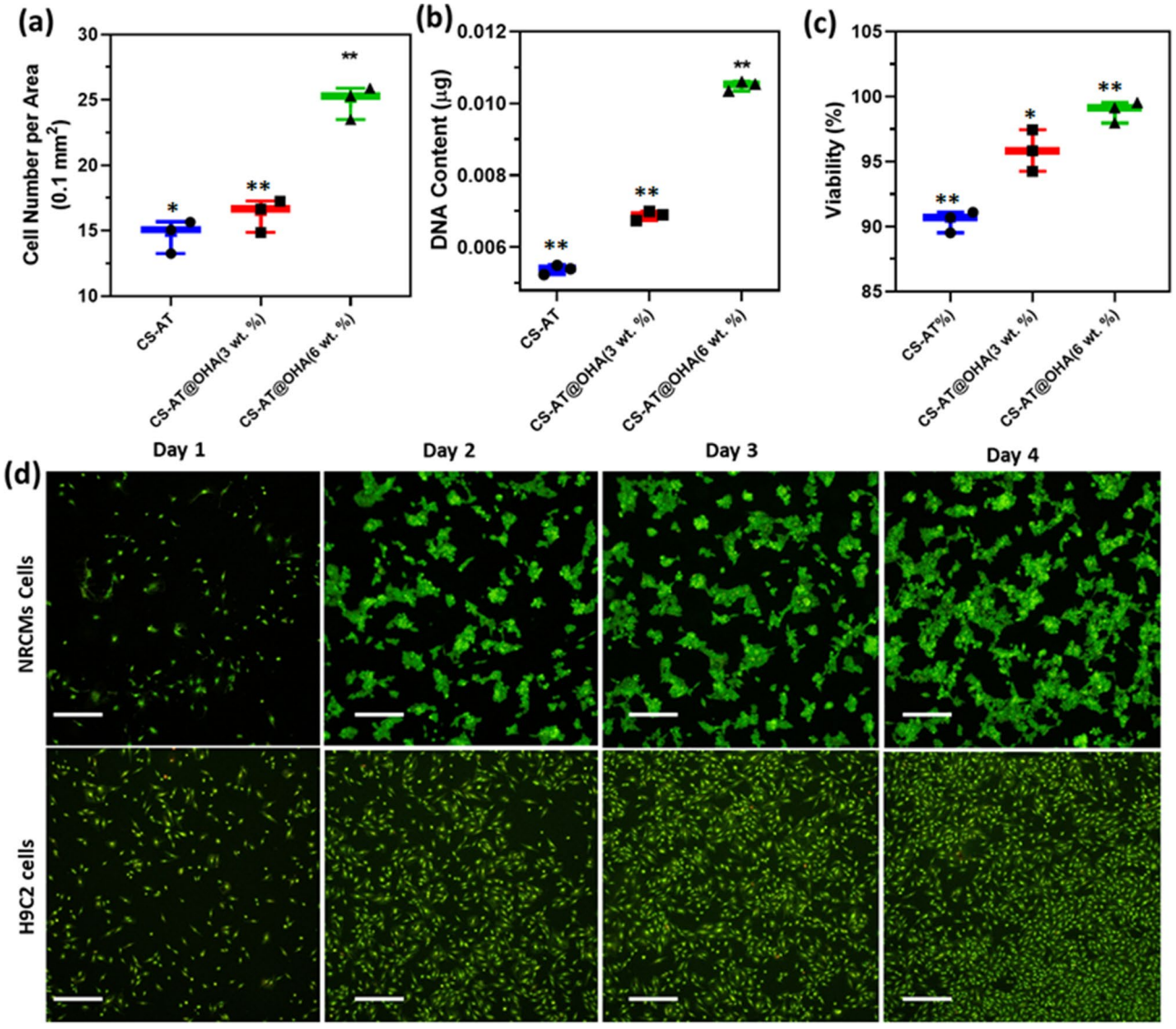

Fig. 4 Analysis of cell viability and cell adhesion of hydrogel samples: (**a**) intracellular cell adhesion of prepared hydrogel groups (CS-AT, CS-AT@OHA (3 %) and CS-AT@OHA (6 %)) by cell counting number per area; (**b**) proliferation ability of the hydrogel samples by quantification of DNA content; (**c**) cell survival rate of the prepared hydrogel samples treated with NRCM cells; Fluorescent microscopic observation of NRCMs and H9C2 cells by AO/EB Live/dead staining treated with prepared hydrogel groups in different incubation days (1, 2, 3 & 4). n = 3 independent experiments per group; *, ** and *** indicate $p < 0.05$, 0.01 and 0.001, respectively

sustained over 90% of cell viability. This observation suggests that the cytotoxicity of the cells was limited. The biological compatibility of the hydrogels was assessed by measuring the proliferation ability of NRCMs and H9C2 cells. According to the findings depicted in Fig. 4 (a, b & c), there was an evident augmentation in the quantity of cells during the course of the three-day culture, as evidenced by the fluorescence microscope images. The quantification of cell counts on various days revealed a significant rise in the number of NRCMs on the second day in comparison to day 1 (Fig. 4 (d)). Furthermore, the upsurge in cell count persisted on the 3 and 4 days. When utilising H9C2 for assessing proliferation within hydrogels, it was observed that the cell counts after a 4-day period exhibited an approximate 50% increase in the CS-AT-OHA hydrogel group. Conversely, there was no discernible increase in cell count within the CS hydrogel group. These findings suggest that the OHA@CS-AT hydrogel significantly enhances the proliferation of H9C2 and NRCMs in comparison to the CS hydrogel. The retention of a specific number of cells within the hydrogel is of significant importance when considering its application as a cell carrier in cardiac cell therapy [65–67]. The hydrogel in question has a dual purpose: it serves as an extracellular matrix to prevent anoikis in cells, while also stimulating cell proliferation. This property is crucial as it

enables a sustained supply of cells for the regeneration of injured cardiac tissues [68, 69].

Injectable hydrogels have gained significant interest in the field of cell treatment, demonstrating their extensive utility. Particularly, injectable conductive hydrogels exhibit considerable promise in the field of cardiac tissue generation [70–72]. In light of the objective to utilise these conductive hydrogels as a means of delivering cells by injection, we conducted additional investigations to assess the survivability of cells within the hydrogels post-injection (Fig. 5a). Hydrogels containing NRCMs and HUCB-MSCs cells at a concentration of 1×10^6 cells mL^{-1} were introduced into the system via 22-gauge needles (Fig. 5b). The number of cells was determined both before and after the injection process. After a duration of 3 h, the examination of the NRCMs and HUCB-MSCs cells revealed no observable alterations subsequent to the injection process (Fig. 5 b). Additionally, there was no noticeable reduction in the quantity of cells within the hydrogel (Fig. 5c), suggesting that the cells maintained a satisfactory level of vitality following the injection. Therefore, the aforementioned conductive hydrogel exhibits significant potential as a viable cell transport platform by intracorporeal injection. Cardiac tissue is comprised of various cellular components. Various sorts of cells were required for the purpose of repairing the heart tissue that had been injured. Stem cells and cardiomyocytes are two distinct cell types that have been extensively employed in the field of cardiac tissue repair [31, 73–75]. In this study, a hydrogel was utilised as a platform for culturing HUCB-MSCs into the hydrogel group, aiming to facilitate the regeneration of cardiac tissue. The cell lines of HUCB-MSCs and NRCMs were individually encapsulated within hydrogels. After a duration of 3 h, it was seen that the cells within various hydrogels exhibited a high level of vitality and were uniformly distributed. This suggests that the hydrogel in question has the potential to serve as an effective medium for encapsulating and mixing diverse cell types. Notably, there was no discernible demarcation between these two cell types. The presence of HUCB-MSCs within the vicinity of NRCMs cells suggests that there was a fusion event between the hydrogels and the migration of cells within the hydrogels. The aforementioned findings also shown that the hydrogel exhibited a favourable capacity for self-healing when it was encapsulated with cells. In the context of repairing injured heart tissue, it is sometimes necessary to utilise multiple types of cells. Consequently, there is a significant demand for carriers capable of encapsulating various cell types within the field of cardiac cell therapy.

The investigation of the cell delivery capabilities of the aforementioned hydrogel groups was performed due to the anticipated utilisation of these self-healing conductive hydrogels in cardiac repair for cell delivery functions. The utilisation of NRCMs cells has been extensively utilised for the process of cardiac tissue restoration. Previous studies have demonstrated that skeletal myoblasts have the capacity to undergo differentiation into myotubes or myocardium, consequently presenting potential for enhancing cardiac performance following an infarction. Therefore, HUCB-MSCs and NRCMs were selected as the cell types to assess the cell distribution capacity of the hydrogels. The experiment covered a duration of seven days, during which the quantities of supplied cells were observed on every day. Different cell types exhibited distinct releasing properties, as illustrated in Fig. 6(a). HUCB-MSCs cells, as compared to NRCMs cells, exhibited an elevated rate of release, likely attributed to the accelerated proliferation of the earlier. The released cell numbers of HUCB-MSCs were found to be influenced by the initial cell number encapsulated in the hydrogel. Specifically, hydrogels with higher cell concentrations embedded in the matrix exhibited a greater release of cells. The findings of this study indicate that the quantity of cells delivered can be efficiently adjusted by modulating the initial cell count. It is noteworthy that the release kinetics of HUCB-MSCs over a period of 4 days and NRCMs cells over a span of 6 days both demonstrated

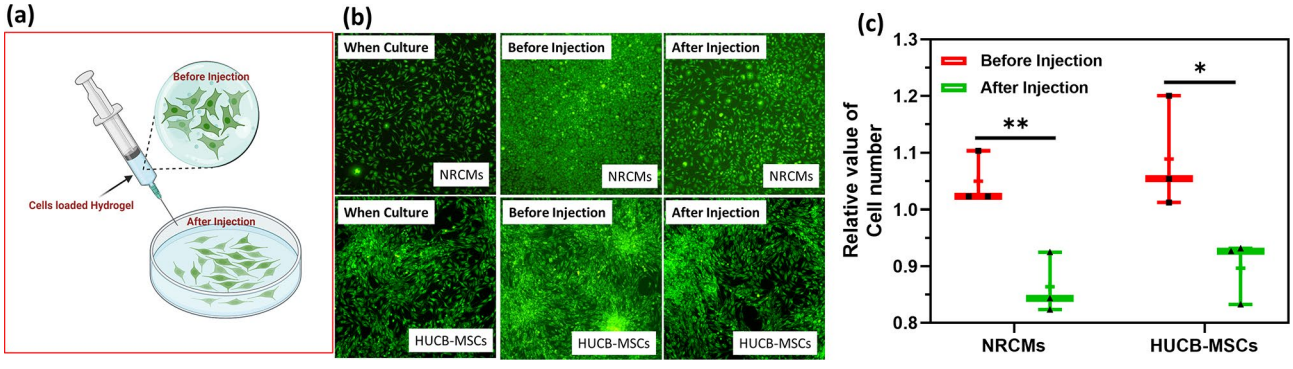

Fig. 5 (**a**) Schematic representation of the MSCs-encapsulated hydrogel for cell injection; (**b**) Fluorescence microscopic images of HUCB-MSCs and NRCMs-encapsulated OHA@CS-AT hydrogel group when culture, before injection and after injection and (**c**) Live cell numbers of HUCB-MSCs and NRCMs before and after injection. n = 3 independent experiments per group; *, ** and *** indicate p & 0.05, 0.01 and 0.001, respectively

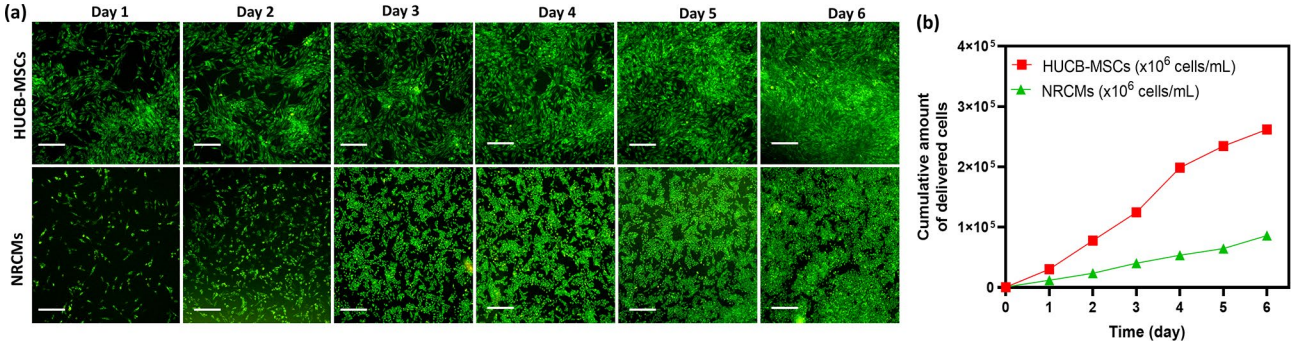

Fig. 6 (**a**) Fluorescence images of different cell types encapsulated with developed hydrogel group for 6 days to observe cell morphology after cell delivery and (**b**) cumulative cell delivery profiles of different cell types loaded with developed hydrogel group. n = 3 independent experiments per group; *, ** and *** indicate $p < 0.05$, 0.01 and 0.001, respectively

a cumulative delivery pattern reflecting proportionality. This observation suggests that these hydrogels possess the potential to offer a consistent supply of cells for the purpose of myocardial tissue repair. In addition to that, prepared hydrogel in presence of HA and CS have appropriate anti-inflammatory efficiency, would be contributed to have immunomodulatory properties to mitigate inflammatory responses, which could be beneficial in reducing the risk of arrhythmias. As previously reported, hyaluronic acid-based hydrogels have an effective anti-inflammatory property, making it beneficial in treating various inflammatory conditions, including osteoarthritis, dermal wounds, and some eye disorders. HA can modulate the activity of various cells involved in the inflammatory process, such as macrophages, leukocytes, and dendritic cells. It can inhibit the production and release of pro-inflammatory cytokines like interleukin-1β (IL-1β) and tumor necrosis factor-alpha (TNF-α), reducing inflammation. In addition to that, HA can act as an antioxidant, scavenging reactive oxygen species (ROS) that are produced in excess during inflammatory processes. By reducing the levels of ROS, HA helps in mitigating oxidative stress and tissue damage. In addition to that, high molecular weight hyaluronic acid is known for its immunosuppressive properties, which can help in reducing the immune response and inflammation. Conversely, low molecular weight HA fragments can have the opposite effect, potentially stimulating an immune response. The anti-inflammatory effects are therefore more associated with high molecular weight HA [76–81].

Echocardiography was employed to evaluate the cardiovascular function of Sprague-Dawley (SD) rats 28 days post-operation. Based on the findings described in Fig. 7, it is evident that the AMI group had notable degeneration and substantial enlargement of infarction. The ejection fraction (EF) and fractional shortening (FS) values exhibited significantly greater magnitudes in the hydrogel-treated groups compared to the MI group. On the other hand, the enhancement in cardiac function in the group treated with conductive CS-AT-OHA hydrogel was more prominent compared to the group treated with CS-AT hydrogel. The inclusion of OHA has the potential to enhance the transmission of electrical impulses inside the region affected by the infarction. There is an increasing number of research indicating that injectable hydrogels may be a viable means of providing mechanical support to damaged cardiac tissue. Figure 7 displays six fundamental factors that characterise cardiac functioning. It was found that there were significant differences in EF (Fig. 7a), FS (Fig. 7b), LVIDd (Fig. 7c), LVIDs (Fig. 7d), EDV (Fig. 7e), and ESV (Fig. 7f) between the five groups and the AMI group. Injectable hydrogels were found to have unique therapeutic benefits, as seen by significant rises in EF and FS and reductions in LVIDd, LVIDs, EDV, and ESV. Among the five distinct hydrogel groups investigated, the CS-AT-OHA hydrogel group exhibited the most favourable therapeutic efficacy in the treatment of the infarcted heart, surpassing the other individual hydrogel groups.

Furthermore, we performed additional observations on the infarct size and fibrosis of the myocardium using the MTS staining method (Fig 8). As illustrated by Fig. 8(A), it can be observed that all regions affected by infarction displayed varying degrees of fibrotic tissue, with the AMI group exhibiting a notable presence of extensive and acute myocardial fibrosis. In contrast, the hydrogel groups displayed a lower degree of fibrosis. The observed results were in agreement with the data obtained from echocardiography. In order to perform a quantitative analysis, we utilised Image J software to determine the infarct size and ventricular wall thickness, drawing upon the data obtained from the MTS approach. The results presented in Fig. 8 (B & C) demonstrate that the application of hydrogel treatments resulted to reduced infarct sizes and increased thickness of the left ventricular (LV) walls. The conductive hydrogel patch is believed to enhance cardiac performance by potentially serving as a bridge between healthy cardiac muscle and

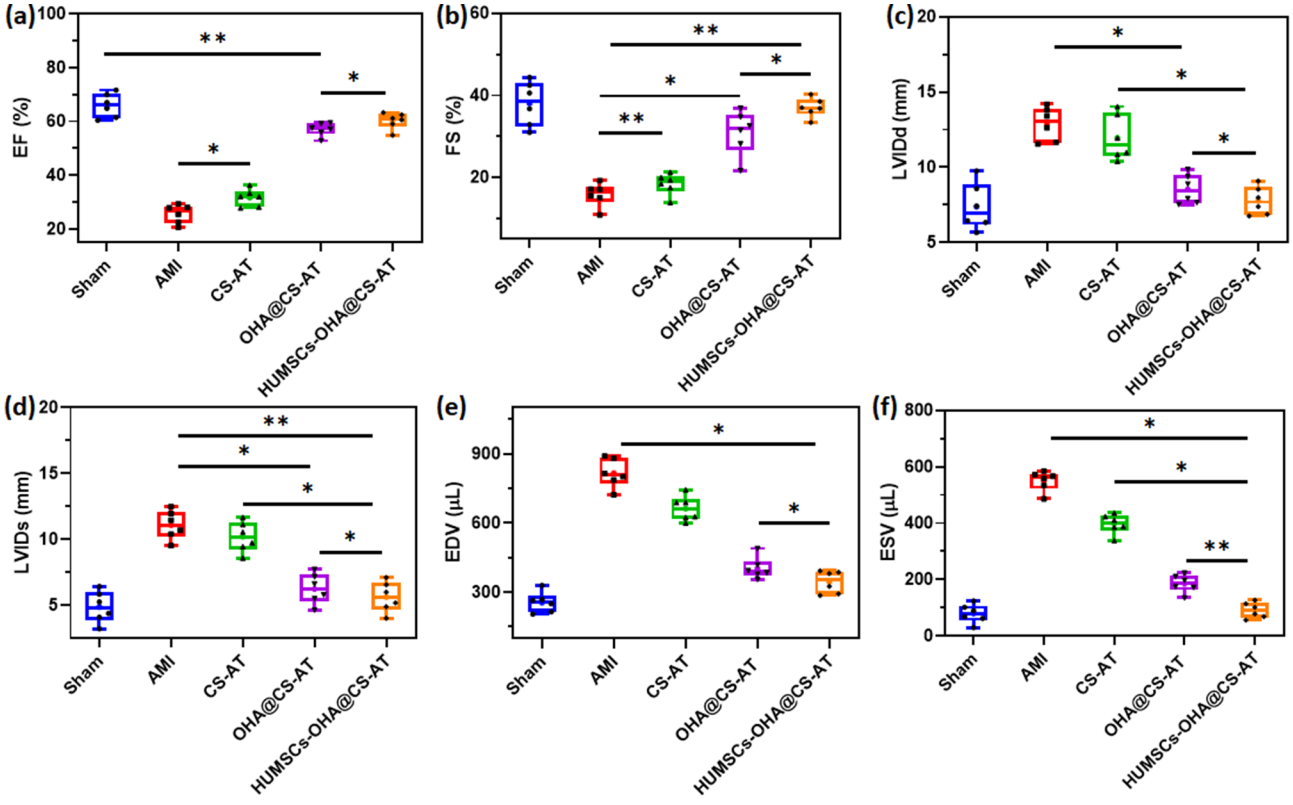

Fig. 7 In vivo cardiac functioning analysis by observation of left ventricular function by echocardiography investigation at 28 days after injection of hydrogel groups. (**a**) EF, (**b**) FS, (**c**) LVIDd, (**d**) LVIDs, (**e**) EDV and (**f**) ESV. *, ** and *** indicate $p < 0.05$, 0.01 and 0.001, respectively

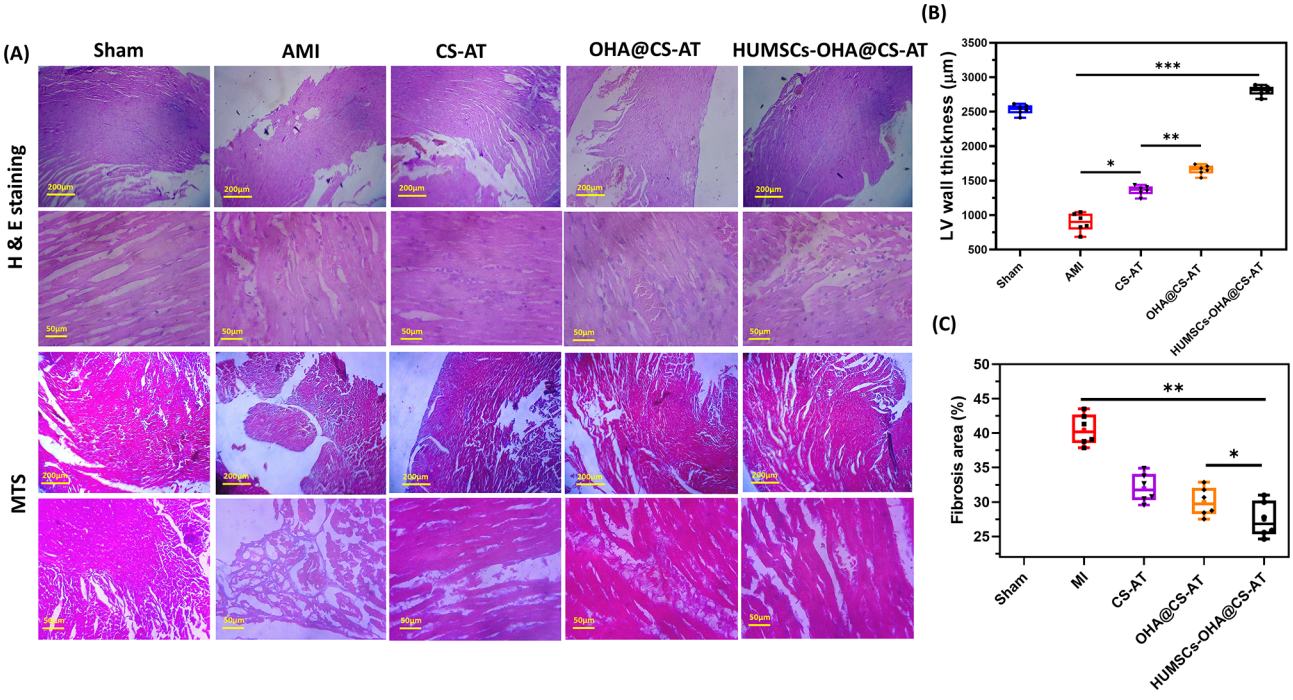

Fig. 8 (**a**) Cardiac morphology of SD rats treated with developed hydrogel groups was observed by histopathological sectioning analysis stained by H & E and MTS (magnifications = 10x and 40x); Quantitative analysis of cardiac morphology was investigated to determine (**b**) LV wall thickness and (**c**) fibrosis area. *, ** and *** indicate $p < 0.05$, 0.01 and 0.001, respectively

viable cardiomyocytes within scar tissue. This bridge may facilitate the propagation of electrical signals across the infarct region, leading to improved cardiac function. Injectable hydrogels have been demonstrated to enhance wall thickness and reduce wall stress, potentially promoting intracellular signalling transduction through mechanoreceptor pathways or aiding in the regulation of tissue repair. Additionally, the electrical conductivity of injectable hydrogels could play a significant role in supporting ventricular remodeling inhibition following myocardial infarction (MI). Ventricular remodeling is a process that occurs after MI, characterized by changes in the size, shape, and function of the heart due to the loss of viable myocardium and the formation of fibrotic scar tissue. This remodeling can lead to heart failure if not properly managed. Injectable conductive hydrogels offer a novel approach to address the challenges of ventricular remodeling through several mechanisms including electrical signal propagation, mechanical support, enhanced cellular environment, therapeutic delivery and direct electrical stimulation. Over all, injectable conductive hydrogels represent a multifaceted therapeutic strategy for addressing post-MI ventricular remodeling. By improving the structural, electrical, and biochemical environment of the damaged heart, these innovative materials hold promise for preserving heart function, preventing heart failure, and improving outcomes for patients with myocardial infarction. Further research and clinical trials are necessary to fully understand their potential and to optimize their composition, conductivity, and delivery methods for maximal therapeutic effect [59, 82–86]. Hence, it is hypothesised that the simultaneous application of an injectable hydrogel has resulted in a significant enhancement of heart function through both external and internal healing mechanisms.

The injectable hydrogel groups exhibit protective effects against myocardial infarction through the activation of many physiological mechanisms, including blood vessel dilation, anti-inflammatory effects, and the promotion of angiogenesis, among others. The study provided evidence that the utilisation of biocompatible injectable hydrogel materials has the capacity to improve the proliferation of MSCs and CMs. The amounts of inflammatory factors (specifically TNF-α) and proangiogenic growth factors (in particular VEGFA and Ang-1 mRNA) in the myocardial tissue were evaluated using qRT-PCR to establish the beneficial effects of injectable hydrogel in the treatment of AMI. Figure 9 (a to f) illustrates that when compared to the AMI group and the other hydrogel groups, the OHA@CS-AT hydrogel group substantially reduces TNF-α expression (Figure 9a) while simultaneously enhancing VEGF (Figure 9b) and Ang-1 (Figure 9c) expression. This is likely due to the ability of OHA-loaded hydrogel to efficiently reduce the adverse microenvironment and enhance cell viability within the AMI region. The above data suggests that hydrogels able to release HUCB-MSCs can inhibit inflammatory reactions and promote angiogenesis, hence contributing to the recovery of heart functions. The Cx43 protein plays an important part in allowing cardiac cells to communicate with one another. The Cx43 expression was examined to identify the consequences of electroactivity during AMI. Figure 9 provides convincing proof that the multifunctional hydrogels induce a substantial up-regulation of Cx43-related mRNA levels. In order to determine the cardiac actions following various therapies, α-SMA and cTnT have been adopted as cardiac biomarkers (Fig. 9). The electrical conductivity of injectable hydrogels could potentially influence the expression of Connexin 43 (Cx43). Cx43 is a protein that forms gap junctions between adjacent cells in cardiac tissue, facilitating the direct electrical communication between cells. This communication is essential for the coordinated contraction of the heart muscle. The expression and localization of Cx43 play a crucial role in maintaining the electrical coupling between cardiomyocytes and, therefore, the overall electrical conductivity of the heart. Injectable hydrogels with electrical conductivity may impact Cx43 expression through various mechanisms. Mainly, enhanced cell-cell communication, electrical stimulation effects, support for cell integration and maturation and promotion of tissue regeneration. The electrical conductivity of hydrogels can facilitate the transmission of electrical signals between cells. This improved communication may positively influence the expression of Cx43, promoting the formation and function of gap junctions between cardiomyocytes. Injectable hydrogels with electrical conductivity may provide a platform for delivering electrical stimulation to the surrounding cardiac tissue. Electrical stimulation has been shown to influence Cx43 expression, potentially promoting the development of gap junctions and enhancing intercellular communication. Conductive hydrogels can create an environment that supports the integration and maturation of newly formed cardiac cells. This may include upregulation of Cx43 expression as cells mature and become more electrically coupled. If the hydrogel supports tissue regeneration and repair, it may contribute to the restoration of Cx43 (Fig. 9d) expression in the damaged myocardium. This is important for maintaining proper electrical conductivity and preventing arrhythmias [50, 84, 87, 88]. The expression levels of α-SMA (Figure 9e) and cTnT (Fig 9f) in the AMI rats are limited. However, following hydrogel injections, particularly in the hydrogel group, there is a notable enhancement in the expression of these two mRNA. This observation indicates a significant enhancement in cardiac function.

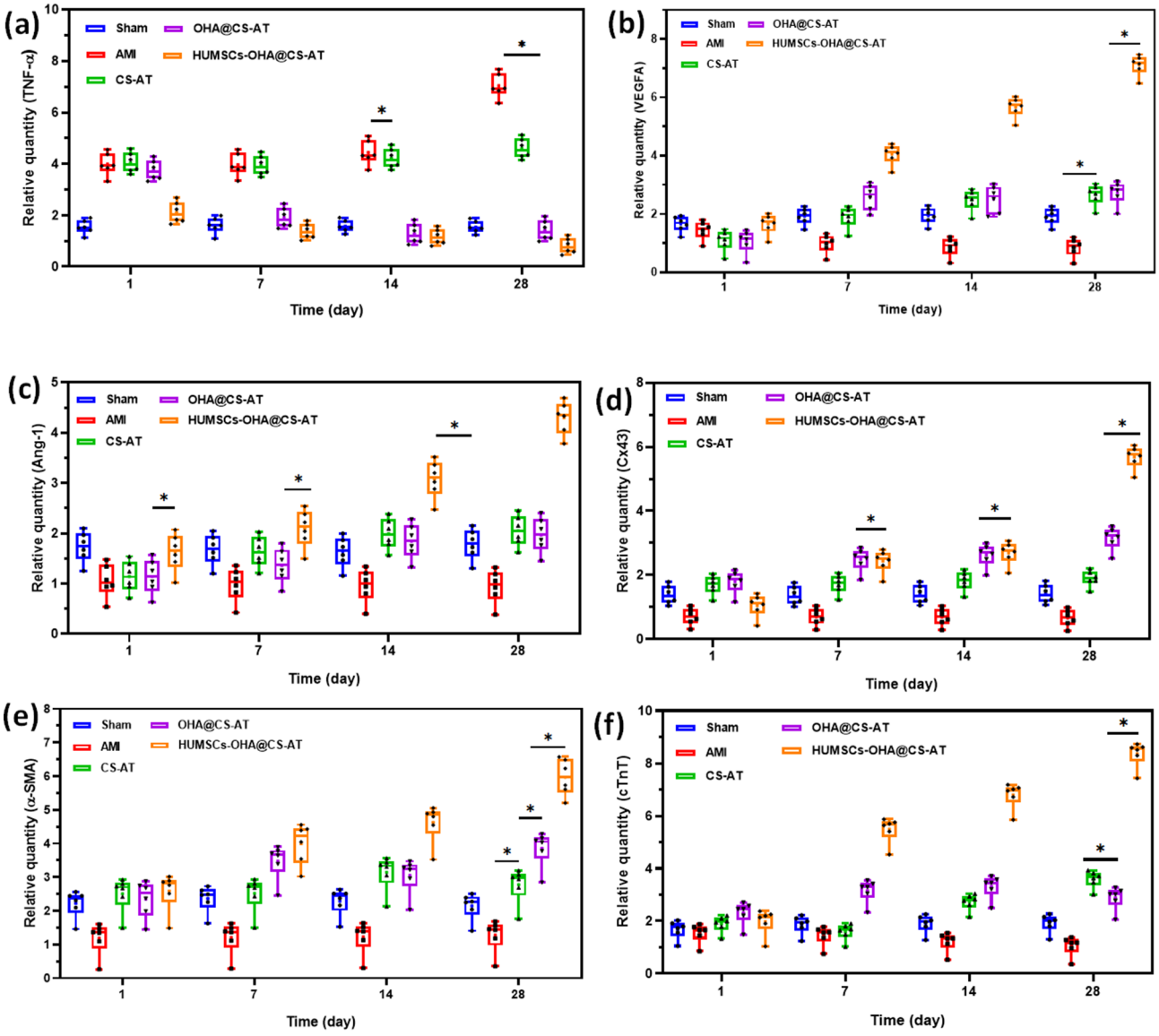

Fig. 9 qRT-PCR analysis was performed to determine relative gene expression profiles of cardiac functioning and regeneration related factors (TNF-α, VEGF, Ang-1, Cx43, α-SMA and cTnT) after 28-day of hydrogel transplanted post-surgery. *, ** and *** indicate $p < 0.05$, 0.01 and 0.001, respectively

To address the complex problem of AMI therapy, we have successfully developed a conductive hydrogel system encapsulated with HUCB-MSC cells for improved AMI therapy. The observed results of physico-chemical characterization and mechanical properties demonstrated that hydrogel have suitable conductivity (2.80×10^{-4} S/cm), optimized gelation and rheological properties which favourable to injectability into heart tissues. In vitro cell analyses revealed that OHA@CS-AT injectable hydrogel have increased cell survival rate (>90%) and proliferation ability with HUCB-MSCs, NRCMs and H9C2 cells, which confirmed the suitability of the hydrogel for AMI treatment. The prepared hydrogels have excellent injectability behavior with damaging implanted cells. In vivo study on AMI-induced SD rat model, prepared HUBC-MSCs loaded hydrogel significantly improved cardiac function and favourable therapeutic efficiency. The results observed from echocardiography and histopathology observation demonstrated the effective restoration from myocardial infarction and improved therapeutic potential in AMI therapy. Importantly, hydrogel treatment in animal models could effectively decreased expressions of inflammatory factors (TNF-α) and increased expressions of proangiogenic growth factor (VEGFA and Ang-1), indicating excellent anti-inflammatory and angiogenic action of hydrogel. On the other hand, the hydrogel could effectively induce the expressions of Cx43, which benefitting to direct electrical communication between cardiac cells. The administration of a multifunctional hydrogel

containing HUCB-MSCs demonstrates a potentially effective therapeutic approach in the treatment of AMI.

Supplementary Information

The online version contains supplementary material available at https://doi.org/10.1186/s13765-024-00904-8.

Supplementary Material 1

Acknowledgements
Not Applicable.

Author contributions
JX contributed to conceptualization, analysis and interpretation of data. YPG contributed to supervision, original draft writing and formatting the manuscript. Both authors read and approved the final manuscript.

Funding
Not Applicable.

Data availability
The datasets used and analyzed during the current study are available from the corresponding author on reasonable request.

Declarations

Competing interests
The authors declare that they have no competing interests.

Received: 23 January 2024 / Accepted: 7 May 2024
Published online: 18 June 2024

References

1. Yao J, Huang K, Zhu D et al (2021) A minimally invasive Exosome Spray repairs Heart after myocardial infarction. ACS Nano 15:11099–11111. https://doi.org/10.1021/acsnano.1c00628
2. Alagarsamy KN, Mathan S, Yan W et al (2021) Carbon nanomaterials for cardiovascular theranostics: promises and challenges. Bioact Mater 6:2261–2280. https://doi.org/10.1016/j.bioactmat.2020.12.030
3. Abbas MM, Abdelmonem HA, Mahmoud AH (2022) Prophylactic effect of Costus and Selenium nanoparticles in Isoproterenol Induced myocardial infarction in rats. Egypt J Hosp Med 89:4817–4823. https://doi.org/10.21608/EJHM.2022.260746
4. Chow A, Stuckey DJ, Kidher E et al (2017) Human Induced Pluripotent Stem Cell-Derived Cardiomyocyte encapsulating bioactive hydrogels improve rat heart function Post myocardial infarction. Stem Cell Rep 9:1415–1422. https://doi.org/10.1016/j.stemcr.2017.09.003
5. Wang H, Liu Z, Li D et al (2012) Injectable biodegradable hydrogels for embryonic stem cell transplantation: improved cardiac remodelling and function of myocardial infarction. J Cell Mol Med 16:1310–1320. https://doi.org/10.1111/j.1582-4934.2011.01409.x
6. Huang P, Wang L, Li Q et al (2020) Atorvastatin enhances the therapeutic efficacy of mesenchymal stem cells-derived exosomes in acute myocardial infarction via up-regulating long non-coding RNA H19. Cardiovasc Res 116:353–367. https://doi.org/10.1093/cvr/cvz139
7. Watson RA, Johnson DM, Dharia RN et al (2020) Anti-coagulant and anti-platelet therapy in the COVID-19 patient: a best practices quality initiative across a large health system. Taylor & Francis
8. Li Q, Hou H, Li M et al (2021) CD73 + mesenchymal stem cells ameliorate myocardial infarction by promoting angiogenesis. Front Cell Dev Biol 9. https://doi.org/10.3389/fcell.2021.637239
9. Wang F, He Y, Yao N et al (2022) Thymosin β 4 protects against Cardiac damage and subsequent Cardiac Fibrosis in mice with myocardial infarction. https://doi.org/10.1155/2022/1308651. Cardiovasc Ther 2022:
10. Gupta S, Kumar S, Sopko N et al (2012) Thymosin β4 and cardiac protection: implication in inflammation and fibrosis. Ann N Y Acad Sci 1269:84–91. https://doi.org/10.1111/j.1749-6632.2012.06752.x
11. Xu Ljiao, Chen R chang, Ma Xyu et al (2020) Scutellarin protects against myocardial ischemia-reperfusion injury by suppressing NLRP3 inflammasome activation. Phytomedicine 68:153169. https://doi.org/10.1016/j.phymed.2020.153169
12. Poh KK, Lee PSS, Djohan AH et al (2020) Transplantation of endothelial progenitor cells in obese Diabetic rats following myocardial infarction: role of Thymosin Beta-4. Cells 9:1–12. https://doi.org/10.3390/cells9040949
13. Liu RF, Gao XY, Liang SW, Zhao HQ (2022) Antithrombotic treatment strategy for patients with coronary artery ectasia and acute myocardial infarction: a case report. World J Clin Cases 10:3936–3943. https://doi.org/10.12998/wjcc.v10.i12.3936
14. Elsayed G (2022) Assessment of nurses' knowledge and practice regarding thrombolytic therapy among patients with Acute myocardial infarction. Trends Nurs Heal Care J 5:62–83. https://doi.org/10.21608/tnhcj.2022.281293
15. Li QL, Tang J, Zhao L et al (2023) The role of CD74 in cardiovascular disease. Front Cardiovasc Med 9:1–14. https://doi.org/10.3389/fcvm.2022.1049143
16. Shen K, Duan A, Cheng J et al (2022) Exosomes derived from hypoxia preconditioned mesenchymal stem cells laden in a silk hydrogel promote cartilage regeneration via the miR-205–5p/PTEN/AKT pathway. Acta Biomater 143:173–188. https://doi.org/10.1016/j.actbio.2022.02.026
17. Zheng Y, Liu J, Chen P et al (2021) Exosomal mir-22-3p from human umbilical cord blood-derived mesenchymal stem cells protects against lipopolysaccharid-induced acute lung injury. Life Sci 269:119004. https://doi.org/10.1016/j.lfs.2020.119004
18. Ma J, Zhao Y, Sun L et al (2017) Exosomes derived from akt -modified human umbilical cord mesenchymal stem cells improve Cardiac Regeneration and promote angiogenesis via activating platelet-derived growth factor D. Stem Cells Transl Med 6:51–59. https://doi.org/10.5966/sctm.2016-0038
19. Ke X, Li M, Wang X et al (2020) An injectable chitosan/dextran/β -glycerophosphate hydrogel as cell delivery carrier for therapy of myocardial infarction. Carbohydr Polym 229:115516. https://doi.org/10.1016/j.carbpol.2019.115516
20. Guilhot F (2020) Human cells for therapeutics purpose: state of the art. Bull Acad Natl Med 204:866–876. https://doi.org/10.1016/j.banm.2020.07.051
21. Wang Z, Wu Z, Liu Y, Han W (2017) New development in CAR-T cell therapy. J Hematol Oncol 10:1–11. https://doi.org/10.1186/s13045-017-0423-1
22. Park JH, Geyer MB, Brentjens RJ (2016) CD19-targeted CAR T-cell therapeutics for hematologic malignancies: interpreting clinical outcomes to date. Blood 127:3312–3320. https://doi.org/10.1182/blood-2016-02-629063
23. Guo R, Wan F, Morimatsu M et al (2021) Cell sheet formation enhances the therapeutic effects of human umbilical cord mesenchymal stem cells on myocardial infarction as a bioactive material. Bioact Mater 6:2999–3012. https://doi.org/10.1016/j.bioactmat.2021.01.036
24. Chen P, Ning X, Li W et al (2022) Fabrication of Tβ4-Exosome-releasing artificial stem cells for myocardial infarction therapy by improving coronary collateralization. Bioact Mater 14:416–429. https://doi.org/10.1016/j.bioactmat.2022.01.029
25. Fish KM, Ishikawa K, Hajjar RJ (2018) Stem cell therapy for acute myocardial infarction: on the horizon or still a dream? Coron Artery Dis 29:89–91. https://doi.org/10.1097/MCA.0000000000000589
26. Carbone RG, Monselise A, Bottino G et al (2021) Stem cells therapy in acute myocardial infarction: a new era? Clin Exp Med 21:231–237. https://doi.org/10.1007/s10238-021-00682-3
27. Zhu D, Wang Y, Thomas M et al (2022) Exosomes from adipose-derived stem cells alleviate myocardial infarction via microRNA-31/FIH1/HIF-1α pathway. J Mol Cell Cardiol 162:10–19. https://doi.org/10.1016/j.yjmcc.2021.08.010
28. Mohammadi Amirabad L, Massumi M, Shamsara M et al (2017) Enhanced Cardiac differentiation of Human Cardiovascular Disease Patient-Specific Induced Pluripotent Stem cells by applying unidirectional electrical pulses using aligned Electroactive Nanofibrous Scaffolds. ACS Appl Mater Interfaces 9:6849–6864. https://doi.org/10.1021/acsami.6b15271
29. Yang S, Zhu B, Yin P et al (2020) Integration of human umbilical cord mesenchymal stem cells-derived exosomes with Hydroxyapatite-embedded Hyaluronic Acid-Alginate Hydrogel for Bone Regeneration. ACS Biomater Sci Eng 6:1590–1602. https://doi.org/10.1021/acsbiomaterials.9b01363
30. Alemdar N, Leijten J, Camci-Unal G et al (2017) Oxygen-Generating Photo-Cross-linkable Hydrogels Support Cardiac Progenitor Cell Survival by reducing Hypoxia-Induced necrosis. ACS Biomater Sci Eng 3:1964–1971. https://doi.org/10.1021/acsbiomaterials.6b00109

31. Shafiq M, Chen Y, Hashim R et al (2021) Reactive oxygen species-based Biomaterials for Regenerative Medicine and tissue Engineering Applications. Front Bioeng Biotechnol 9:1–9. https://doi.org/10.3389/fbioe.2021.821288
32. Shafiq M, Jung Y, Kim SH (2016) Insight on stem cell preconditioning and instructive biomaterials to enhance cell adhesion, retention, and engraftment for tissue repair. Biomaterials 90:85–115. https://doi.org/10.1016/j.biomaterials.2016.03.020
33. Serpooshan V, Zhao M, Metzler SA et al (2013) The effect of bioengineered acellular collagen patch on cardiac remodeling and ventricular function post myocardial infarction. Biomaterials 34:9048–9055. https://doi.org/10.1016/j.biomaterials.2013.08.017
34. Tang J, Cui X, Caranasos TG et al (2017) Heart Repair using Nanogel-Encapsulated Human Cardiac Stem cells in mice and pigs with myocardial infarction. ACS Nano 11:9738–9749. https://doi.org/10.1021/acsnano.7b01008
35. Xu G, Wang X, Deng C et al (2015) Injectable biodegradable hybrid hydrogels based on thiolated collagen and oligo(acryloyl carbonate)-poly(ethylene glycol)-oligo(acryloyl carbonate) copolymer for functional cardiac regeneration. Acta Biomater 15:55–64. https://doi.org/10.1016/j.actbio.2014.12.016
36. Hu C, Liu W, Long L et al (2022) Regeneration of infarcted hearts by myocardial infarction-responsive injectable hydrogels with combined anti-apoptosis, anti-inflammatory and pro-angiogenesis properties. Biomaterials 290. https://doi.org/10.1016/j.biomaterials.2022.121849
37. Wu C, Zhang Y, Xu Y et al (2023) Injectable polyaniline nanorods/alginate hydrogel with AAV9-mediated VEGF overexpression for myocardial infarction treatment. Biomaterials 296:122088. https://doi.org/10.1016/j.biomaterials.2023.122088
38. Ding H, Ding J, Liu Q et al (2022) Mesenchymal stem cells encapsulated in a reactive oxygen species-scavenging and O2-generating injectable hydrogel for myocardial infarction treatment. Chem Eng J 433:133511. https://doi.org/10.1016/j.cej.2021.133511
39. Wang Z, Hu C, Zhang W et al (2023) An injectable ECM-like hydrogel with bioactive peptides and RepSox nanoparticles for myocardial infarction treatment. Chem Eng J 474:145878. https://doi.org/10.1016/j.cej.2023.145878
40. Lin S, Zhu Y, Hu T et al (2023) Novel design of nano-selenium loaded injectable hydrogel combined with mesenchymal stem cells-derived exosomes improving cardiac repair and nursing care after acute myocardial infarction. J Drug Deliv Sci Technol 87:104711. https://doi.org/10.1016/j.jddst.2023.104711
41. Li P, Hu J, Wang J et al (2023) The role of Hydrogel in Cardiac Repair and Regeneration for myocardial infarction: recent advances and future perspectives. https://doi.org/10.3390/bioengineering10020165. Bioengineering 10:
42. Chen J, Han X, Deng J et al (2021) An injectable hydrogel based on phenylboronic acid hyperbranched macromer encapsulating gold nanorods and astragaloside IV nanodrug for myocardial infarction. Chem Eng J 413:127423. https://doi.org/10.1016/j.cej.2020.127423
43. Liu Y, Guo R, Wu T et al (2021) One zwitterionic injectable hydrogel with ion conductivity enables efficient restoration of cardiac function after myocardial infarction. Chem Eng J 418:129352. https://doi.org/10.1016/j.cej.2021.129352
44. Gao H, Liu S, Qin S et al (2024) Injectable hydrogel-based combination therapy for myocardial infarction: a systematic review and Meta-analysis of preclinical trials. BioMed Central
45. Naderi-Meshkin H, Andreas K, Matin MM et al (2014) Chitosan-based injectable hydrogel as a promising in situ forming scaffold for cartilage tissue engineering. Cell Biol Int 38:72–84. https://doi.org/10.1002/cbin.10181
46. Cheng Y-H, Chen Y-C, Yang S-H et al (2010) Thermosensitive chitosan – gelatin – glycerol phosphate hydrogels as a cell carrier for Nucleus Pulposus. TISSUE Eng Part A 16:695–703
47. Xu Y, Cui M, Patsis PA et al (2019) Reversibly assembled Electroconductive Hydrogel via a host-Guest Interaction for 3D cell culture. ACS Appl Mater Interfaces 11:7715–7724. https://doi.org/10.1021/acsami.8b19482
48. Ye L, Zhang W, Su LP et al (2011) Nanoparticle based delivery of hypoxia-regulated VEGF transgene system combined with myoblast engraftment for myocardial repair. Biomaterials 32:2424–2431. https://doi.org/10.1016/j.biomaterials.2010.12.008
49. Dai J, Long W, Liang Z et al (2018) A novel vehicle for local protein delivery to the inner ear: injectable and biodegradable thermosensitive hydrogel loaded with PLGA nanoparticles. Drug Dev Ind Pharm 44:89–98. https://doi.org/10.1080/03639045.2017.1373803
50. Wang W, Tan B, Chen J et al (2018) An injectable conductive hydrogel encapsulating plasmid DNA-eNOs and ADSCs for treating myocardial infarction. Biomaterials 160:69–81. https://doi.org/10.1016/j.biomaterials.2018.01.021
51. Ding J, Yao Y, Li J et al (2020) A reactive oxygen species scavenging and O2 Generating Injectable Hydrogel for myocardial infarction treatment in vivo. Small 16:1–9. https://doi.org/10.1002/smll.202005038
52. Wu Y, Chang T, Chen W et al (2021) Release of VEGF and BMP9 from injectable alginate based composite hydrogel for treatment of myocardial infarction. Bioact Mater 6:520–528. https://doi.org/10.1016/j.bioactmat.2020.08.031
53. Mushtaq I, Mushtaq I, Akhter Z et al (2020) Engineering electroactive and biocompatible tetra(aniline)-based terpolymers with tunable intrinsic antioxidant properties in vivo. Mater Sci Eng C 108:110456. https://doi.org/10.1016/j.msec.2019.110456
54. Dong R, Zhao X, Guo B, Ma PX (2016) Self-Healing Conductive Injectable hydrogels with Antibacterial Activity. as Cell Delivery Carrier for Cardiac Cell Therapy
55. Lyu Y, Xie J, Liu Y et al (2020) Injectable Hyaluronic Acid Hydrogel loaded with Functionalized Human mesenchymal stem cell aggregates for repairing Infarcted Myocardium. ACS Biomater Sci Eng 6:6926–6937. https://doi.org/10.1021/acsbiomaterials.0c01344
56. Liang W, Chen J, Li L et al (2019) Conductive hydrogen sulfide-releasing hydrogel encapsulating ADSCs for myocardial infarction treatment. ACS Appl Mater Interfaces 11:14619–14629. https://doi.org/10.1021/acsami.9b01886
57. Gao Q, Xie W, Wang Y et al (2018) A theranostic nanocomposite system based on radial mesoporous silica hybridized with Fe3O4 nanoparticles for targeted magnetic field responsive chemotherapy of breast cancer. RSC Adv 8:4321–4328. https://doi.org/10.1039/c7ra12446e
58. Wu T, Cui C, Huang Y et al (2020) Coadministration of an Adhesive Conductive Hydrogel Patch and an Injectable Hydrogel to treat myocardial infarction. ACS Appl Mater Interfaces 12:2039–2048. https://doi.org/10.1021/acsami.9b17907
59. Wu T, Liu W (2022) Functional hydrogels for the treatment of myocardial infarction. NPG Asia Mater. https://doi.org/10.1038/s41427-021-00330-y. 14:
60. Li H, Gao J, Shang Y et al (2018) Folic acid derived Hydrogel enhances the survival and promotes therapeutic efficacy of iPS cells for Acute myocardial infarction. ACS Appl Mater Interfaces 10:24459–24468. https://doi.org/10.1021/acsami.8b08659
61. Fiorica C, Palumbo FS, Pitarresi G et al (2020) A hyaluronic acid/cyclodextrin based injectable hydrogel for local doxorubicin delivery to solid tumors. Int J Pharm 589:119879. https://doi.org/10.1016/j.ijpharm.2020.119879
62. Chen X, Zhu L, Wang X, Xiao J (2023) Insight into Heart-Tailored Architectures of Hydrogel to restore Cardiac functions after myocardial infarction. Mol Pharm 20:57–81. https://doi.org/10.1021/acs.molpharmaceut.2c00650
63. Srisuk P, Berti FV, Da Silva LP et al (2018) Electroactive Gellan Gum/Polyaniline spongy-like Hydrogels. ACS Biomater Sci Eng 4:1779–1787. https://doi.org/10.1021/acsbiomaterials.7b00917
64. Bertuoli PT, Ordono J, Armelin E et al (2019) Electrospun Conducting and Biocompatible Uniaxial and Core-Shell fibers having poly(lactic acid), poly(ethylene glycol), and Polyaniline for Cardiac tissue Engineering. ACS Omega 4:3660–3672. https://doi.org/10.1021/acsomega.8b03411
65. French KM, Boopathy AV, Dequach JA et al (2012) A naturally derived cardiac extracellular matrix enhances cardiac progenitor cell behavior in vitro. Acta Biomater 8:4357–4364. https://doi.org/10.1016/j.actbio.2012.07.033
66. Shi C, Li Q, Zhao Y et al (2011) Stem-cell-capturing collagen scaffold promotes cardiac tissue regeneration. Biomaterials 32:2508–2515. https://doi.org/10.1016/j.biomaterials.2010.12.026
67. An Z, Tian J, Liu Y et al (2022) Exosomes as a cell-free therapy for myocardial Injury following Acute myocardial infarction or ischemic reperfusion. Aging Dis 13:1770–1786. https://doi.org/10.14336/AD.2022.0416
68. Cui H, Liu Y, Cheng Y et al (2014) In vitro study of electroactive tetraaniline-containing thermosensitive hydrogels for cardiac tissue engineering. Biomacromolecules 15:1115–1123. https://doi.org/10.1021/bm4018963
69. Yuan Z, Qin Q, Yuan M et al (2020) Development and novel design of clustery graphene oxide formed Conductive Silk hydrogel cell vesicle to repair and routine care of myocardial infarction: investigation of its biological activity for cell delivery applications. J Drug Deliv Sci Technol 60:102001. https://doi.org/10.1016/j.jddst.2020.102001
70. Li J, Lv Y, Zhu D et al (2022) Intrapericardial hydrogel injection generates high cell retention and augments therapeutic effects of mesenchymal stem cells in myocardial infarction. Chem Eng J 427:131581. https://doi.org/10.1016/j.cej.2021.131581
71. Atluri P, Miller JS, Emery RJ et al (2014) Tissue-engineered, hydrogel-based endothelial progenitor cell therapy robustly revascularizes ischemic myocardium and preserves ventricular function. J Thorac Cardiovasc Surg 148:1090–1098. https://doi.org/10.1016/j.jtcvs.2014.06.038

72. Fu H, Fu J, Ma S et al (2020) An ultrasound activated oxygen generation nanosystem specifically alleviates myocardial hypoxemia and promotes cell survival following acute myocardial infarction. J Mater Chem B 8:6059–6068. https://doi.org/10.1039/d0tb00859a
73. Davis ME, Hsieh PCH, Takahashi T et al (2006) Local myocardial insulin-like growth factor 1 (IGF-1) delivery with biotinylated peptide nanofibers improves cell therapy for myocardial infarction. Proc Natl Acad Sci U S A 103:8155–8160. https://doi.org/10.1073/pnas.0602877103
74. Song Y, Wang B, Zhu X et al (2021) Human umbilical cord blood–derived MSCs exosome attenuate myocardial injury by inhibiting ferroptosis in acute myocardial infarction mice. Cell Biol Toxicol 37:51–64. https://doi.org/10.1007/s10565-020-09530-8
75. Wang J, Pei B, Yan J et al (2022) HucMSC-Derived exosomes alleviate the deterioration of Colitis via the miR-146a/SUMO1 Axis. Mol Pharm 19:484–493. https://doi.org/10.1021/acs.molpharmaceut.1c00450
76. Tarricone E, Mattiuzzo E, Belluzzi E et al (2020) Anti-inflammatory performance of lactose-modified Chitosan and Hyaluronic Acid mixtures in an in vitro macrophage-mediated inflammation osteoarthritis model. https://doi.org/10.3390/cells9061328. Cells 9:
77. Qiu B, Gong M, He QT, Zhou PH (2016) Controlled release of interleukin-1 receptor antagonist from hyaluronic acid-chitosan microspheres attenuates interleukin-1 β -induced inflammation and apoptosis in chondrocytes. Biomed Res Int 2016:. https://doi.org/10.1155/2016/6290957
78. Jin Y, Koh RH, Kim SH et al (2020) Injectable anti-inflammatory hyaluronic acid hydrogel for osteoarthritic cartilage repair. Mater Sci Eng C 115:111096. https://doi.org/10.1016/j.msec.2020.111096
79. altman-et-al-2018- anti-inflammatory-effects-of-intra-articular-hyaluronic-acid-a-systematic-review.pdf
80. Kaderli S, Boulocher C, Pillet E et al (2015) A novel biocompatible hyaluronic acid-chitosan hybrid hydrogel for osteoarthrosis therapy. Int J Pharm 483:158–168. https://doi.org/10.1016/j.ijpharm.2015.01.052
81. Ito T, Fraser IP, Yeo Y et al (2007) Anti-inflammatory function of an in situ cross-linkable conjugate hydrogel of hyaluronic acid and dexamethasone. Biomaterials 28:1778–1786. https://doi.org/10.1016/j.biomaterials.2006.12.012
82. Liu Z, Wang H, Wang Y et al (2012) The influence of chitosan hydrogel on stem cell engraftment, survival and homing in the ischemic myocardial microenvironment. Biomaterials 33:3093–3106. https://doi.org/10.1016/j.biomaterials.2011.12.044
83. Zhu S, Yu C, Liu N et al (2022) Injectable conductive gelatin methacrylate / oxidized dextran hydrogel encapsulating umbilical cord mesenchymal stem cells for myocardial infarction treatment. Bioact Mater 13:119–134. https://doi.org/10.1016/j.bioactmat.2021.11.011
84. Zhang L, Bei Z, Li T, Qian Z (2023) An injectable conductive hydrogel with dual responsive release of rosmarinic acid improves cardiac function and promotes repair after myocardial infarction. Bioact Mater 29:132–150. https://doi.org/10.1016/j.bioactmat.2023.07.007
85. Navaei A, Rahmani Eliato K, Ros R et al (2019) The influence of electrically conductive and non-conductive nanocomposite scaffolds on the maturation and excitability of engineered cardiac tissues. Biomater Sci 7:585–595. https://doi.org/10.1039/c8bm01050a
86. Wei X, Chen S, Xie T et al (2022) An MMP-degradable and conductive hydrogel to stabilize HIF-1α for recovering cardiac functions. Theranostics 27:127–142. https://doi.org/10.7150/THNO.63481
87. You JO, Rafat M, Ye GJC, Auguste DT (2011) Nanoengineering the heart: conductive scaffolds enhance connexin 43 expression. Nano Lett 11:3643–3648. https://doi.org/10.1021/nl201514a
88. Navaei A, Moore N, Sullivan RT et al (2017) Electrically conductive hydrogel-based micro-topographies for the development of organized cardiac tissues. RSC Adv 7:3302–3312. https://doi.org/10.1039/C6RA26279A

Publisher's Note